Loveringite from the Last-Yavr mafic-ultramafic intrusion, Kola Peninsula; a second occurrence in Russia

ANDREW Yu. BARKOV, YEVGENY E. SAVCHENKO, YURII P. MEN'SHIKOV & LARISSA P. BARKOVA

Barkov, A. Yu., Savchenko, Ye. E., Men'shikov, Yu, P. & Barkova, L. P.: Loveringite from the Last-Yavr mafic-ultramafic intrusion, Kola Peninsula; a second occurrence in Russia. *Norsk Geologisk Tidsskrift*, Vol. 76, pp. 115–120. Oslo 1996. ISSN 0029-196X.

Loveringite, (Ca, REE)(Ti, Fe, Cr)$_{21}$O$_{38}$ (a member of the crichtonite group) occurs in orthocumulates (plagioclase-bearing orthopyroxenites) of the Last-Yavr intrusion, which obviously represents a fragment of the Proterozoic Fedorova Tundra-Pana Tundra layered intrusion. The occurrence is situated immediately adjacent to the Archaean wall rocks at a lower structural level of the intrusion. The loveringite is closely associated with a typical intercumulus assemblage (phlogopite, quartz, albite-rich plagioclase, ilmenite, rutile and Ca-amphibole). Its composition is characterized by a relatively low content of REE and high concentrations of Cr and Mg. The reflectance values are in good agreement with published data; VHN$_{100}$ = 912–1085. The unit-cell dimensions are a = 10.40 (3), c = 20.83 (6) Å.

A. Yu. Barkov, Ye. E. Savchenko, Yu. P. Men'shikov & L. P. Barkova, Geological Institute, Kola Science Centre, Russian Academy of Sciences, 14 Fersman Street, 184200 Apatity, Russia. *Present address: Department of Geosciences and Astronomy, University of Oulu, FIN-90570 Oulu, Finland.*

Introduction

Loveringite, (Ca, REE)(Ti, Fe, Cr)$_{21}$O$_{38}$, a rare member of the crichtonite group, was first described by Gatehouse et al. (1978) from the Early Proterozoic Jimberlana layered intrusion, Australia. The mineral has also been discovered in the Bushveld layered complex, South Africa (Cameron 1978; 1979), and later in several Early Proterozoic mafic-ultramafic layered intrusions in Finland: Näränkävaara, Penikat (Alapieti 1982; Alapieti & Lahtinen 1986) and Koitelainen (Tarkian & Mutanen 1987). Another Fennoscandian occurrence of members of the loveringite-davidite series was reported by Olerud (1988) from an Early Proterozoic albite felsite, Norway. Segalstad (1984) described an unusual Ti-rich oxide mineral, the chemistry of which resembles that of the crichtonite group. Lorand et al. (1987) reported an occurrence of loveringite from the Early Palaeozoic Laouni complex, Algeria. More recently, loveringite was identified in the Burakovsky layered intrusion, Russian Karelia (Barkov et al. 1994). Minerals of the loveringite-crichtonite series have also been found in the Khibina alkaline complex, Kola Peninsula, Russia (Barkov et al., in prep.).

In this paper we report a second Russian occurrence of loveringite, from the Last-Yavr intrusion, Kola Peninsula.

Brief geological description

The Last-Yavr mafic-ultramafic intrusion is situated in the central part of the Kola Peninsula, at the contact between the better known Fedorova Tundra and Pana Tundra intrusions (Fig. 1). The intrusions are located between Archaean granitoids and the Palaeoproterozoic Seidorechensky volcanogenic-sedimentary sequence. Fea-

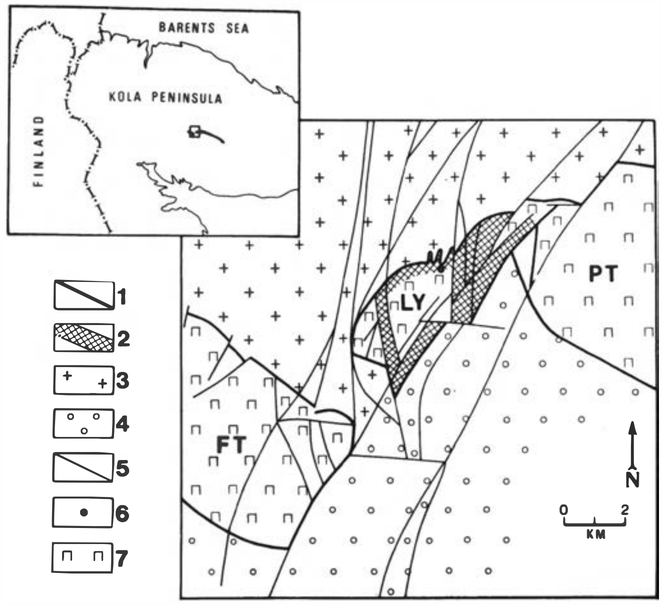

Fig. 1. Simplified geological sketch-map of the contact area between the Fedorova Tundra and Pana Tundra layered intrusions, showing location of the Last-Yavr intrusive body. Modified from Radchenko et al. (1980) *1.* Geological contacts; *2.* Schists and mylonites after mafic and ultramafic rocks; *3.* Archaean granitoids; *4.* Palaeoproterozoic Seidorechensky complex of volcanic and sedimentary rocks; *5.* Faults; *6.* Position of drill hole No. 72; *7.* Mafic-ultramafic igneous rocks. Abbreviations used: FT = Fedorova Tundra, PT = Pana Tundra, LY = Last-Yavr intrusions. The inset shows the approximate location of the area on the Kola Peninsula.

Table 1. Representative electron microprobe analyses (in wt.%) of minerals in loveringite-bearing pyroxenite from Last-Yavr.

	En	Aug	Pl		Phl	Am	Ap		Chr
			core	rim					
SiO_2	55.17	52.99	59.06	60.30	40.41	48.10	n.a.	n.a.	n.d.
TiO_2	0.15	0.62	n.d.	n.d.	2.63	0.40	n.a.	n.a.	0.30
Al_2O_3	1.17	2.27	25.57	25.85	14.55	11.38	n.a.	n.a.	9.82
Cr_2O_3	0.33	0.64	n.d.	n.d.	0.71	0.10	n.a.	n.a.	43.18
V_2O_3	n.d.	0.04	n.d.	n.d.	0.05	n.d.	n.a.	n.a.	0.74
Fe_2O_3	–	–	–	–	–	–	–	–	11.75
FeO	10.81	6.18	0.12	0.10	5.89	7.71	0.19	0.24	29.61
MnO	0.27	0.17	n.d.	n.d.	0.04	0.13	n.a.	n.a.	0.45
MgO	30.70	18.65	n.d.	n.d.	22.65	17.05	n.a.	n.a.	1.32
CaO	1.14	17.32	7.10	7.13	0.04	10.79	54.64	54.39	n.d.
SrO	n.a.	n.a.	n.a.	n.a.	n.a.	n.a.	0.11	n.d.	n.a.
Na_2O	0.16	0.46	7.21	8.07	0.47	2.10	n.a.	n.a.	n.a.
K_2O	n.d.	n.d.	0.03	0.03	8.61	0.10	n.a.	n.a.	n.a.
Ce_2O_3	n.a.	n.a.	n.a.	n.a.	n.a.	n.a.	0.21	0.12	n.a.
NiO	0.09	0.05	n.a.	n.a.	0.13	0.06	n.a.	n.a.	n.d.
ZnO	n.a.	n.a.	n.a.	n.a.	n.a.	n.a.	n.a.	n.a.	0.84
P_2O_5	n.a.	n.a.	n.a.	n.a.	n.a.	n.a.	42.08	42.30	n.a.
Cl	n.a.	n.a.	n.a.	n.a.	n.d.	0.06	1.45	1.56	n.a.
Cl-O	–	–	–	–	–	0.01	0.33	0.36	–
Total	99.99	99.39	99.09	101.48	96.18	97.97	98.35	98.25	98.01
					Number of cations				
	O=6		O=8		O=11	O=23	O=12.5		O=4
Si	1.94	1.94	2.65	2.65	2.85	6.80	–	–	–
Ti	<0.01	0.02	–	–	0.14	0.04	–	–	<0.01
Al	0.05	0.10	1.35	1.34	1.21	1.90	–	–	0.42
Cr	<0.01	0.02	–	–	0.04	0.01	–	–	1.24
V	–	<0.01	–	–	<0.01	–	–	–	0.02
Fe^{3+}	0.06	<0.01	–	–	–	–	–	–	0.32
Fe^{2+}	0.26	0.19	<0.01	<0.01	0.35	0.91	0.01	0.02	0.90
Mn	<0.01	<0.01	–	–	<0.01	0.02	–	–	0.01
Mg	1.61	1.02	–	–	2.38	3.59	–	–	0.07
Ca	0.04	0.68	0.34	0.34	<0.01	1.63	4.95	4.92	–
Sr	–	–	–	–	–	–	<0.01	–	–
Ce	–	–	–	–	–	–	<0.01	<0.01	–
Na	0.01	0.03	0.63	0.69	0.07	0.58	–	–	–
K	–	–	<0.01	<0.01	0.77	–	–	–	–
Ni	<0.01	<0.01	–	–	<0.01	<0.01	–	–	–
Zn	–	–	–	–	–	–	–	–	0.02
P	–	–	–	–	–	–	3.01	3.02	–
Cl	–	–	–	–	–	–	0.21	0.22	–

Abbreviations: En = enstatite, Aug = augite, Pl = plagioclase, Phl = phlogopite, Am = amphibole, Ap = apatite, Chr = chromite (a euhedral grain enclosed within enstatite). Total Fe as FeO; Fe^{3+} in chromite was calculated assuming stoichiometry; Fe^{3+} in pyroxenes is from a program by Cebriá Gómez (1990).
n.d. = not detected; n.a. = not analysed.

tures of the regional geology shown in Fig. 1 strongly suggest that the Last-Yavr intrusion represents a block of the Fedorova Tundra-Pana Tundra intrusion, rather than an individual layered intrusion. There are no published age determinations for the Last-Yavr body, but it may be considered to have a Proterozoic age, in common with the Fedorova Tundra, Pana Tundra and other comparable layered intrusions in the Kola Peninsula, Russian Karelia and Finland.

Table 2. Electron microprobe analyses (in wt.%) of ilmenite and rutile from Last-Yavr.

	Ilmenite				Rutile	
	1*	2*	3*	4**	5*	6*
TiO_2	53.77	52.81	53.72	52.61	97.86	98.14
FeO	42.53	44.23	42.44	42.46	0.16	0.10
Cr_2O_3	n.d.	n.d.	n.d.	n.d.	0.72	0.62
Al_2O_3	n.d.	n.d.	n.d.	n.d.	0.06	0.05
MgO	2.05	1.85	2.18	2.14	0.27	0.16
MnO	0.62	0.58	0.65	1.72	n.d.	n.d.
Total	98.97	99.47	98.99	98.93	99.07	99.07

* Individual grains, ** a rim around loveringite.
Total Fe as FeO.

Descriptions of the Last-Yavr geology were given by Radchenko et al. (1980) and Bartenev et al. (1980, 1981). The geological information is based on drilling and geophysical work as the intrusion is wholly covered by Quaternary deposits. The intrusion is a small body (approximately 10 km^2 in surface area) that has undergone intensive regional deformation and was broken up by tectonic movements to form several blocks (Fig. 1). In general, the thickness of the intrusion increases towards the Pana Tundra intrusion. The original cumulates are either only locally preserved or completely altered, due to strong deformation and metamorphism, and relatively fresh rocks are present in subordinate amounts. The

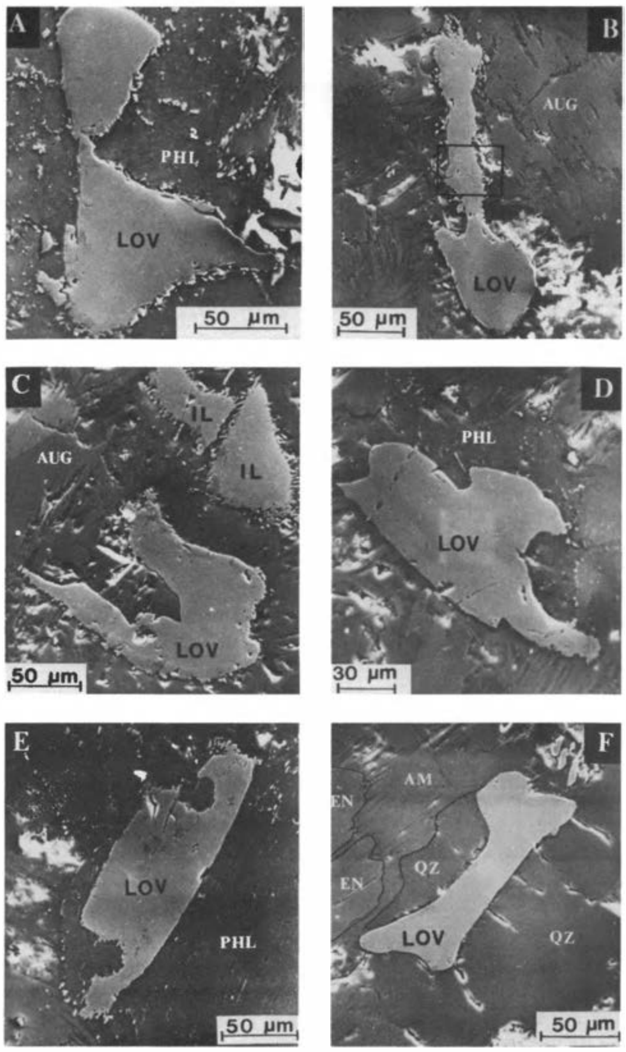

Fig. 2. The Last-Yavr loveringite and its textural relationships with associated minerals. Secondary electron images. White spots are due to local polish defects. **A:** anhedral loveringite (LOV) enclosed within intercumulus phlogopite (PHL); **B, C:** anhedral elongated and irregular loveringite grains (LOV) occurring adjacent to augite (AUG). IL = ilmenite. Details of the outlined area in Fig. 2B are shown in Fig. 3; **D, E:** anhedral loveringite (LOV) intergrown with phlogopite (PHL); **F:** irregular grain of loveringite (LOV) hosted by quartz (QZ). AM = Ca-amphibole, En = enstatite.

fresh orthopyroxene cumulates were observed in samples from borehole No. 72, some of which were chosen for this study. Relatively slightly altered rocks were also encountered in both the southern and southwestern parts of the intrusion. Fine-grained marginal rocks (quartz-bearing gabbronorites; thickness up to 20–25 m), occurring there in the contact zone with Archaean country rocks, contain xenoliths of staurolite- and sillimanite-bearing gneisses (Radchenko et al. 1980). The fine-grained gabbronorites are overlain by inhomogeneous gabbronorites, which may be considered to belong to the marginal series of the intrusion.

On the whole, the lowermost part of the Last-Yavr layered series is composed of predominantly plagioclase-bearing orthopyroxenites. The upper part is formed mainly by meta-gabbronorites and meta-gabbros. The

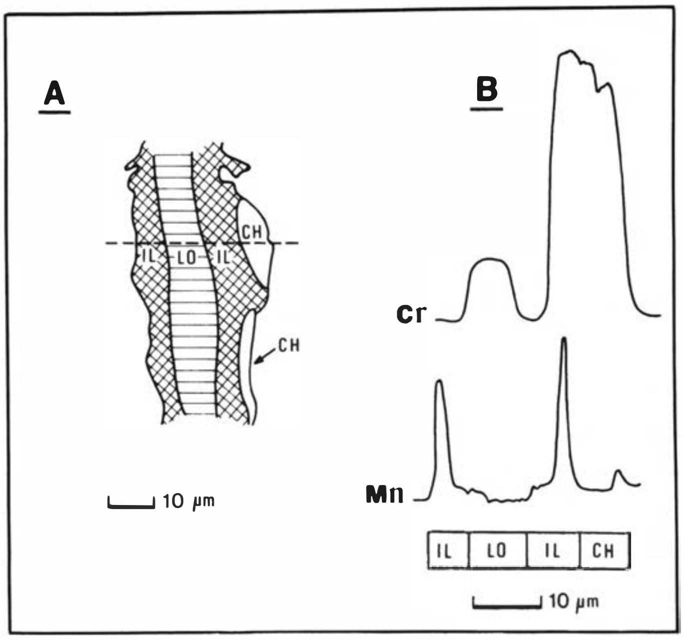

Fig. 3. **A:** Sketch of a part of the loveringite grain shown in Fig. 2B (drawn from a polished section). Note that loveringite (LO) is mantled by Mn-bearing ilmenite (IL), that is rimmed by chromite (CH). **B:** Chromium (Cr) and manganese (Mn) distribution profile across the composite grain. The path of this profile is shown in Fig. 3A. Abbreviations are the same as in Fig. 3A. Scale bars each represent 10 μm.

total thickness of mafic-ultramafic cumulates in the intrusion reaches ca. 1 km.

Several Cu-Ni sulphide deposits have been found in the Last-Yavr intrusion (Bartenev et al. 1980, 1981).

Petrography and mineralogy

The Last-Yavr loveringite occurs in plagioclase-bearing pyroxenite at the northern margin of the intrusion. The mineral was identified in sample No. 72/305.45 from drill hole No. 72, cutting the orthopyroxenitic sequence adjacent to the wall rocks (Fig. 1). As mentioned, the rocks are fresh. If classified according to cumulate terminology, the pyroxenite represents orthocumulate containing approximately 80 vol.% of orthopyroxene. The composition of cumulus orthopyroxene was found to be nearly constant ($Wo_{2.2-2.8}En_{80.8-81.7}Fs_{16.1-16.4}$). Ca-rich pyroxene (up to 3–4 vol.%) is represented by augite ($Wo_{35.9}E_{53.8}Fs_{10.3}$) that is locally poikilitic. Intercumulus plagioclase (< 10 vol.%) has a high albite content and a distinct compositional zonation. One grain exhibits zoning from Ab_{63} in the core area to Ab_{69} in the rim (Table 1). A rather coarse-grained quartz (up to 1.5 mm across) is present in significant amounts in the intercumulus spaces, where it is generally intergrown with phlogopite and andesine. Results of microprobe analysis of phlogopite are presented in Table 1. Intercumulus ilmenite (Fig. 2), rutile and apatite are common accessory minerals. Apatite forms relatively large anhedral grains (up to 0.3 mm). Its chlorine content does not exceed 1.6 wt.%.

Table 3. Electron microprobe analyses of loveringite from Last-Yavr.

	Weight %				No. of atoms*		
	1	2	3		1	2	3
TiO_2	60.84	60.11	61.64	Ca	0.96	0.97	0.98
Fe_2O_3	16.95	16.90	15.96	Ce	0.11	0.11	0.10
Cr_2O_3	9.37	9.32	9.32	La	0.08	0.08	0.07
SiO_2	0.16	0.23	0.22	Nd	0.02	0.02	0.02
Al_2O_3	0.98	1.00	1.11	U	–	0.01	–
MgO	1.14	1.13	1.85	Th	<0.01	0.02	0.02
MnO	0.15	0.13	0.11	Σ	1.17	1.21	1.19
CaO	3.04	3.06	3.15				
ZnO	0.05	0.05	n.d.	Ti	13.45	13.40	13.43
ZrO_2	3.84	3.89	3.76	Fe^{3+}	3.75	3.77	3.48
V_2O_3	0.59	0.54	0.65	Cr	2.18	2.18	2.14
La_2O_3	0.77	0.75	0.70	Mg	0.50	0.50	0.80
Ce_2O_3	1.01	1.05	0.96	Al	0.34	0.35	0.38
Nd_2O_3	0.20	0.20	0.17	Si	0.05	0.07	0.06
UO_2	n.d.	0.15	n.d.	Zr	0.55	0.56	0.53
ThO_2	0.08	0.24	0.29	V	0.14	0.13	0.15
				Mn	0.04	0.03	0.03
Total	99.17	98.75	99.89	Zn	0.01	0.01	–
				Σ	21	21	21

* Number of atoms was calculated on the basis of $\Sigma Ti + Fe^{3+} + Cr + Mg + Al + Si + Zr + V + Mn + Zn = 21$.
Total Fe as Fe_2O_3.

Individual ilmenite grains (Table 2) show a relatively high content of MgO (up to 2.2 wt.%), whereas their MnO concentrations (up to 0.65 wt.%) are much less than that detected in an ilmenite rim around loveringite (about 1.7 wt.%). However, Mn is distributed very inhomogeneously in the rim. Rims of the Mn-bearing ilmenite around loveringite grains commonly occur in Last-Yavr, as well as in Finnish layered intrusions (e.g. Alapieti 1982; Tarkian & Mutanen 1987). This contrasts with textural observations from the Burakovsky layered intrusion, where ilmenite is rimmed by loveringite (Barkov et al. 1994).

The Last-Yavr loveringite is accompanied by ilmenite and rutile. Chromite is also present, but is rare. Two different generations of chromite are clearly identified microscopically and compositionally. The first is represented by euhedral to subhedral, small (typically up to 50 μm across) inclusions in orthopyroxene. The chromite of the second generation occurs both as thin rims around ilmenite and as small grains located in the outermost areas of such composite intergrowths. An example is shown in Fig. 3. It demonstrates that loveringite is surrounded by this ilmenite. The intercumulus assemblage also includes a Ca-amphibole that locally replaces the orthopyroxene (e.g. Fig. 2F).

Loveringite is not a rare mineral in this occurrence. For instance, more than 10 grains of loveringite were found in a polished section. It appears as anhedral grains intimately associated with phlogopite, quartz and other intercumulus minerals (Fig. 2). Most of the grains are no larger than 0.1 mm, but grains reaching 0.15 mm in length were also encountered. All the observed grains occupy a distinctly interstitial position.

In addition, scattered base-metal sulphide minerals (predominantly chalcopyrite and pyrite) occur as minute grains (typically < 50 μm in diameter).

Table 4. X-ray powder data (in Å) for loveringite from Last-Yavr.

I	$d_{meas.}$	$d_{calc.}$	hkl
3	4.16	4.162	113
2	3.74	3.714	015
4	3.39	3.406	024
1	3.20	3.236	122
3	3.05	3.058	205
7	2.887	2.888	116
2	2.760	2.756	033
1	2.631	2.636	125
9	2.479	2.480	311
1	2.429	2.429	312
5	2.253	2.252	314
9	2.144	2.142	315
3	1.911	1.913	317
6	1.803	1.803	318
2	1.712	1.710	146
10	1.600	1.600	3 1 10
4	1.509	1.509	3 1 11
10	1.444	1.444	2 2 12

Reflectance, microhardness and composition

The reflectance measurements were performed on a MSFP-2 microphotometer with a silicon standard. The diameter of the measured field was approximately 4–5 μm. The following reflectance values in air were obtained: 470 nm 17.1%; 546 nm 16.2%; 589 nm 16.0%; 650 nm 15.9%. These values are in good agreement with those published by Tarkian & Mutanen (1987) and Barkov et al. (1994). Previously, Kelly et al. (1979) reported only one reflectance value in air in white light (R = 17%).

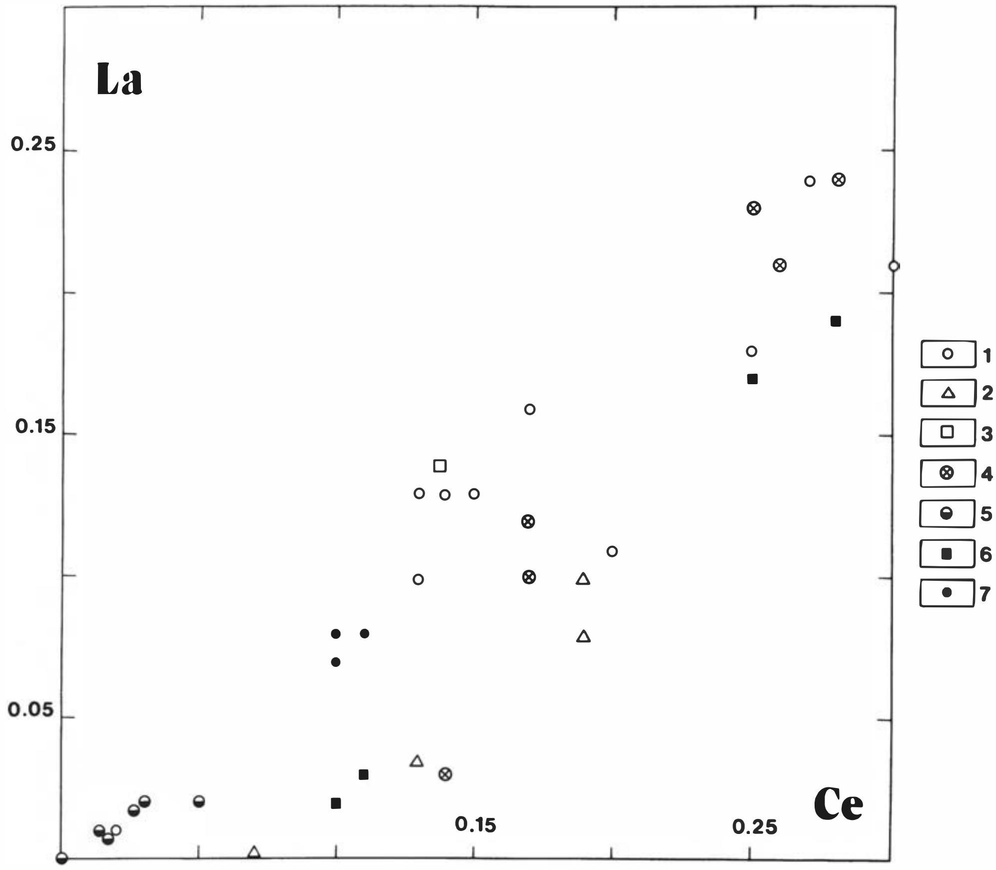

Fig. 4. La content of loveringites shown versus their Ce content on the basis of atoms per 38 oxygens. The loveringites are from the following localities: *1.* from Jimberlana (Campbell & Kelly 1978); *2.* from Bushveld (Cameron 1979); *3.* from Koillismaa (Alapieti 1982); *4.* from Koitelainen (Tarkian & Mutanen 1987); *5.* from Laouni (Lorand et al. 1987); *6.* from Burakovsky (Barkov et al. 1994); *7.* from Last-Yavr (this study).

There is a great discrepancy between the results of loveringite microhardness measurements reported in the literature: $VHN_{10} = 421-464$ (Kelly et al. 1979) and $VHN_{100} = 792-933$ (Tarkian & Mutanen 1987). Microhardness measurements carried out for the Burakovsky loveringite ($VHN_{40} = 1010-1060$) are in good accord with values obtained by Tarkian & Mutanen (1987). The Last-Yavr loveringite yields the microhardness values $VHN_{100} = 912-1085$ that are in good agreement with those reported by Tarkian & Mutanen (1987) and Barkov et al. (1994). Measurement errors might have been responsible for the low microhardness values published by Kelly and co-authors.

Loveringite was analysed at the Geological Institute, Kola Science Centre, Russian Academy of Sciences, using a Cameca electron microprobe operated at 22 kV (31 kV for Zr, U and Th), sample current either 20 or 40 nA. The standards used are the same as those described by Barkov et al. (1994).

Results of the analyses obtained for three different grains are listed in Table 3. All grains are chemically rather homogeneous or only slightly inhomogeneous. The compositions are comparable to those reported from other occurrences, but the REE content of the Last-Yavr loveringites is markedly lower, and concentrations of Cr and Mg are higher than those of many other loveringites reported in the literature (Table 3; Fig. 4). Figure 4 demonstrates that there is a rather strong positive correlation between La and Ce in loveringite.

X-ray powder study

The material analysed by X-ray powder diffraction is from an individual grain shown in Fig. 2A. It was extracted from a polished section and analysed using a 57.3 mm Debye-Scherrer camera and FeKα radiation; intensities were estimated visually. Reflections (Table 4) of the Last-Yavr loveringite are similar to those of loveringite from other occurrences. The powder pattern was indexed on the basis of a hexagonal cell, in agreement with the cell parameters reported by Lorand et al. (1987). The unit-cell parameters of the Last-Yavr loveringite refined by least squares from the powder pattern are a = 10.40(3), c = 20.83(6) Å.

Concluding remarks

The Last-Yavr loveringite occurrence resembles the Burakovsky occurrence (Barkov et al. 1994) in that it is located immediately adjacent to Archaean wall rocks. Both occurrences imply that conditions favouring loveringite crystallization may be typically attained at contact zones between mafic-ultramafic intrusions and felsic country rocks, both in their layered and marginal series.

Like other reported occurrences, loveringite from Last-Yavr occurs in orthocumulates and is intimately associated with typical intercumulus assemblages. Textural relationships indicate that loveringite crystallized before Mn-bearing ilmenite and postcumulus chromite, which form composite rims around loveringite. Our interpretation of the origin of these rims is the same as that presented by Tarkian & Mutanen (1987), who concluded that the rims were produced through a reaction of loveringite with residual intercumulus liquid.

It seems very unlikely that the loveringite geochemistry may be taken as a good indicator for the degree of differentiation of parental magmas. However, we cannot exclude that higher concentrations of incompatible elements (REE, Zr) and lower of Cr and Mg may be reasonably expected in loveringites crystallized from more evolved (fractionated) magmas.

Two possibilities may be considered to explain the appearance of abundant REE-bearing phases in the lower cumulates, in the vicinity of the contact zone, in the Last-Yavr intrusion. The first is that magmatic contamination might have been responsible for relative REE enrichment of the mineral-forming environment. This is consistent with the presence of numerous xenoliths in the marginal series of the intrusion (Radchenko et al. 1980). It is noteworthy that salic xenoliths of many types are also common in contact zones of several neighbouring Finnish layered intrusions (Alapieti et al. 1990). Besides, the lead isotopic composition of galenas from the marginal series of one of the Finnish intrusions (Suhanko-Konttijärvi) provides strong evidence for the magmatic contamination. The second possibility is that relative enrichments in REE and other incompatible elements were characteristic compositional features of the Last-Yavr parental magma. More data are required to support one of these possibilities.

Acknowledgements. – We extend our thanks to Drs. T. T. Alapieti, G. Raade and T. V. Segalstad for constructive and helpful reviews, and Dr. R. Boyd, Editor, for valuable suggestions for improving the manuscript. This work was supported by the International Science Foundation through grant RLY000 to AYuB, and the Russian Foundation for Basic Research through grant 95-05-16503 σ to YuPM. We thank M. Radchenko for providing the Last-Yavr samples. Thanks are also extended to Drs. Ya. A. Pakhomovskii and Yu. N. Neradovskii for the microhardness and reflectance measurements, respectively.

Manuscript received October 1994

References

Alapieti, T. 1982: The Koillismaa layered igneous complex, Finland – its structure, mineralogy and geochemistry, with emphasis on the distribution of chromium. *Geological Survey of Finland, Bulletin* 319, 116 pp.

Alapieti, T. T. & Lahtinen, J. J. 1986: Stratigraphy, petrology, and platinum-group element mineralization of the Early Proterozoic Penikat layered intrusion, northern Finland. *Economic Geology* 81, 1126–1136.

Alapieti, T. T., Lahtinen, J. J., Huhma, H., Hänninen, E., Piirainen, T. A. & Sivonen, S. J. 1989: *In* Prendergast, M. D. & Jones, M. J. (eds.): *Magmatic Sulphides, The Zimbabwe Volume, The Institution of Mining and Metallurgy,* 177–187. London.

Alapieti, T. T., Filén, B. A., Lahtinen, J. J., Lavrov, M. M., Smolkin, V. F. & Voitsekhovsky, S. N. 1990: Early Proterozoic layered intrusions in the northeastern part of the Fennoscandian Shield. *Mineralogy and Petrology 42,* 1–22.

Barkov, A. Yu., Pakhomovskii, Ya. A., Trofimov, N. N. & Lavrov, M. M. 1994: Loveringite: a first occurrence in Russia, from the Burakovsky layered intrusion, Karelia. *Neues Jahrbuch für Mineralogie, Monatshefte* 3, 101–111.

Bartenev, I. S., Klimentiev, V. N. & Tel'nov, V. A. 1980: Geological structure and sulphide copper-nickel mineralization of the Last-Yavr deposit. *In Geology and Structure of Ore Deposits in the Kola Peninsula,* 75–81. Geological Institute, Kola Science Centre, Apatity (in Russian).

Bartenev, I. S., Klimentiev, V. N. & Tel'nov, V. A. 1981: New data on the geology of the Last-Yavr copper-nickel sulphide deposit. *In Geology of Ore Deposits in the Kola Peninsula,* 3–10. Geological Institute, Kola Science Centre, Apatity (in Russian).

Cameron, E. N. 1978: An unusual titanium-rich oxide mineral from the Eastern Bushveld Complex. *American Mineralogist 63,* 37–39.

Cameron, E. N. 1979: Titanium-bearing oxide minerals of the Critical Zone of the Eastern Bushveld Complex. *American Mineralogist 64,* 140–150.

Campbell, I. H. & Kelly, P. R. 1978: The geochemistry of loveringite, a uranium-rare-earth-bearing accessory phase from the Jimberlana Intrusion of Western Australia. *Mineralogical Magazine 42,* 187–193.

Cebriá Gómez, J. M. 1990: PX: A program for pyroxene classification and calculation of end-members. *American Mineralogist 75,* 1426–1427.

Gatehouse, B. M., Grey, I. E., Campbell, I. H. & Kelly, P. 1978: The crystal structure of loveringite – a new member of the crichtonite group. *American Mineralogist 63,* 28–36.

Kelly, P. R., Campbell, I. H., Grey, I. E. & Gatehouse, B. M. 1979: Additional data on loveringite (Ca, REE)(Ti, Fe, Cr)$_{21}$O$_{38}$ and mohsite discredited. *Canadian Mineralogist 17,* 635–638.

Lorand, J.-P., Cottin, J.-Y. & Parodi, G. C. 1987: Occurrence and petrological significance of loveringite in the Western Laouni Complex, southern Hoggar, Algeria. *Canadian Mineralogist 25,* 683–693.

Olerud, S. 1988: Davidite-loveringite in early Proterozoic albite felsite in Finnmark, north Norway. *Mineralogical Magazine 52,* 400–402.

Radchenko, M. K., Borisova, V. V. & Dokuchaeva, V. S. 1980: *In Formation Analysis of the Basic-ultrabasic Rocks in the Middle Part of the Kola Peninsula* 65–73. Geological Institute, Kola Science Centre, Apatity (unpublished report; in Russian).

Segalstad, T. V. 1984: An unusual titanium-rich oxide mineral from Oslo, Norway. *American Mineralogist 69,* 388–390.

Tarkian, M. & Mutanen, T. 1987: Loveringite from the Koitelainen Layered Intrusion, Northern Finland. *Mineralogy and Petrology 37,* 37–50.